Flame propagation under partially-premixed conditions

By G. R. Ruetsch

1. Motivation and objectives

In combustion, flames are generally categorized according to the distribution of reactants in the flow. For homogeneous mixtures of fuel and oxidizer, flames are designated as premixed, and when the fuel and oxidizer are initially separated, non-premixed or diffusion flames arise. There are many instances when flames clearly fall in one of these two categories, such as premixed flames in internal combustion engines and diffusion flames during later stages of combustion in diesel engines.

There are, however, many practical situations where flames cannot be considered as purely premixed or non-premixed. One important phenomenon that occurs in such partially-premixed conditions concerns how diffusion flames are stabilized in mixing layers. Through the imbalance between chemical source and diffusion, premixed flames can propagate into unburned regions, whereas diffusion flames by themselves have no such propagation mechanism. Therefore, some degree of premixing is necessary for diffusion flame stabilization. Liñán 1994 shows that there are two possibilities for stabilization of diffusion flames in laminar mixing layers. The flame can either be stabilized near the splitter plate or stabilized farther downstream, as a lifted flame. In the former case the flame is anchored in the wake of the splitter plate, and the velocity deficit of the wake and heat conduction to the plate play important roles in stabilization and must be taken into account. These anchored flames have been examined by Veynante *et al.* 1994. In the case of the lifted flame these mechanisms are absent, and laminar flame stabilization is achieved through "triple flames," i.e. a flame composed of two premixed flames, one fuel rich and the other lean, and a trailing diffusion flame. The two premixed wings provide the ability to propagate, and the diffusion wing provides an anchor for the trailing diffusion flame.

In addition to regions where diffusion flame stabilization takes place, partially-premixed conditions also exist during the ignition process in nonpremixed systems. Numerical simulations by Réveillon *et al.* 1994 of the ignition process in a weakly stirred mixture of fuel and oxidizer show that triple flames propagate along lines of stoichiometric mixture fraction throughout the fluid. In addition, Peters 1994 notes that NO_x emissions are likely to be large in such transient cases, and therefore an understanding of triple flames can provide beneficial information concerning pollutant formation.

One of the first observations of triple flames was made by Phillips 1965, where he investigated a triple flame propagating in a methane mixing layer. More recently, Kioni *et al.* 1993 have analyzed triple flames both experimentally and numerically. In their numerical approach, they first develop a model for triple flames in a counterflow geometry under the assumption of zero heat release and then solve these

equations numerically to analyze the structure and propagation of these flames. There have also been numerous analytical studies of triple flames under various assumptions by Dold 1989, Dold *et al.* 1991, and Hartley and Dold 1991.

This study concentrates on developing a better understanding of triple flames. More precisely, we relax the assumption of zero heat release which has been used in many of the previously mentioned analytical studies. The effects of heat release in turbulent mixing layers have been previously studied by McMurtry *et al.* 1989, where the influence of heat release on the large-scale structures, entrainment, and other properties of shear layers has been analyzed. However, such simulations are temporal and do not address the issues of stabilization and flame propagation. In order to investigate the role heat release plays in flame propagation in partially-premixed combustion, we return to a simple flow field and investigate the behavior of flames in a laminar environment.

1.1 Numerical simulation and flow configuration

We use direct numerical simulations to solve the fully-compressible Navier-Stokes equations in this investigation. The simulation used is a two-dimensional version of the code previously developed by Trouve 1991. This code uses the high-order compact finite difference scheme of Lele 1992 for spatial differentiation, the third order Runge-Kutta scheme of Wray for time advancement, and the Navier-Stokes characteristic boundary conditions method of Poinsot and Lele 1992. Below we summarize some of the important features and assumptions of the code relevant to this work; for further details on the numerical method readers are referred to Lele 1992 and Poinsot and Lele 1992.

The chemical scheme we consider is represented by a one-step global reaction between a fuel and oxidizer:

$$F + O \longrightarrow P$$

where we have assumed unity stoichiometric coefficients for simplicity. The reaction rate behaves according to the Arrhenius form:

$$\dot{w} = K\rho Y_F \rho Y_O \exp\left(-\frac{T_{ac}}{T}\right)$$

where ρ is the density, T_{ac} is the activation temperature, K is the pre-exponential factor, and Y_F and Y_O are the fuel and oxidizer mass fractions. Following Williams 1986, we can write this reaction rate as

$$\dot{w} = \Lambda\rho Y_F \rho Y_O \exp\left(-\frac{\beta(1-\theta)}{1-\alpha(1-\theta)}\right)$$

where the reduced pre-exponential factor(Λ), heat release parameter(α), Zel'dovich number(β), and reduced temperature(θ) are defined by:

$$\Lambda = K\exp(-\beta/\alpha); \quad \alpha = \frac{T_f - T_0}{T_f}; \quad \beta = \frac{\alpha T_{ac}}{T_f}; \quad \theta = \frac{T - T_0}{T_f - T_0}$$

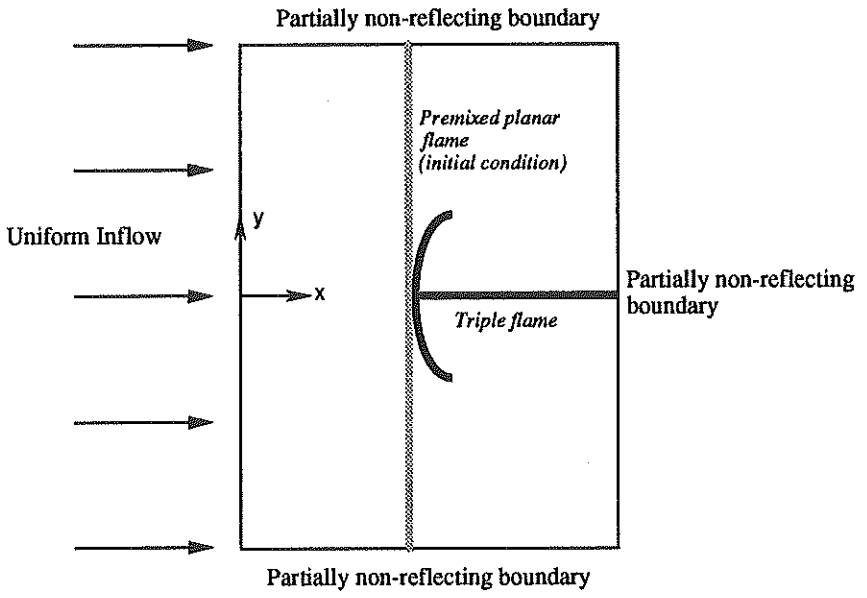

FIGURE 1. Computational domain used in the simulations.

with T_f being the adiabatic flame temperature and T_0 taken in the ambient flow. In this study we hold the Zel'dovich number constant at $\beta = 8$ and use heat release parameters of $\alpha = 0.5$, $2/3$, 0.75, and 0.8.

The transport coefficients in the simulations are temperature dependent. This temperature dependence is expressed through the molecular viscosity, μ, given by:

$$\mu = \mu_0 \left(\frac{T}{T_0} \right)^a$$

with $a = 0.76$. The temperature dependence of the thermal conductivity, λ, and the mass diffusivities, $\mathcal{D}_k$, is obtained by requiring the Lewis and Prandtl numbers to be constant:

$$Le_k = \frac{\lambda}{\rho \mathcal{D}_k c_p}; \qquad Pr = \frac{\mu c_p}{\lambda},$$

where $k = F, O$ refers to either the fuel or or oxidizer species. We assume unity Lewis numbers throughout this study.

We solve the compressible Navier-Stokes equations in a two-dimensional domain depicted in Fig. 1. At the boundaries we use an inflow boundary condition on the left and nearly-perfect reflective boundary conditions, required to avoid pressure drift, at the outflow and sides. Although the inflow conditions are prescribed, values can

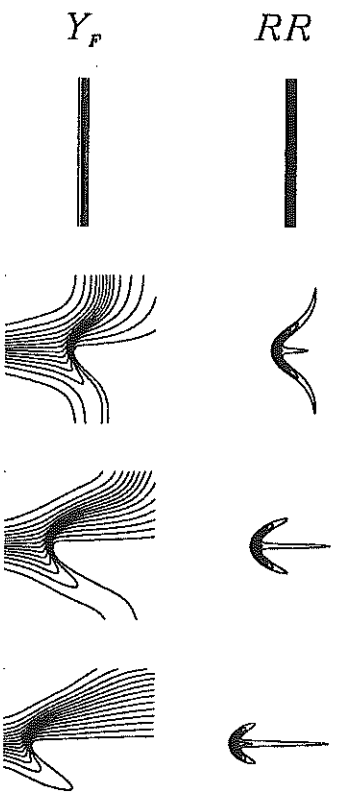

FIGURE 2. Response of a planar premixed flame to a mixture fraction gradient. The first row in the time sequence shows the premixed flame in a steady-state situation. As the mixture fraction gradient reaches the flame, the structure and velocity of the flame change.

be changed during the simulation. Within this domain we initialize the flow with a planar premixed flame where the mixture fraction, defined as

$$Z = \frac{1 + Y_F - Y_O}{2},$$

is everywhere equal to its stoichiometric value, $Z_s = 0.5$. The incoming flow is uniform and set equal to the premixed laminar flame speed, S_L^0. Also associated with the flame is the premixed flame thickness, δ_L^0.

After the flow and flame are initialized, the mixture fraction is varied at the inlet from its uniform stoichiometric value to a tanh profile varying from zero to one. We characterize the thickness of this mixing layer by the slope of the profile at

stoichiometric conditions and the overall change in mixture fraction, which gives:

$$\delta_M(x) = \Delta Z \left(\left. \frac{\partial Z}{\partial y} \right|_{y=0} \right)^{-1} = \left(\left. \frac{\partial Z}{\partial y} \right|_{y=0} \right)^{-1}$$

It is important to realize that this measure does not remain constant along the stoichiometric line and is a function of x. We can form a Damköhler number using the mixing thickness and the planar flame thickness. Since the characteristic velocity for both chemical and physical processes is the same, we can simply define the Damköhler number as:

$$D = \frac{\tau_p}{\tau_c} = \frac{\delta_M}{\delta_L^0},$$

which can be thought of as a dimensionless mixing thickness. The mixing thickness used in this expression is evaluated at the location of the maximum reaction rate.

An example of a flame's response to a variable mixture fraction is shown in Fig. 2. With the uniform flow approaching from the left, as the mixture fraction gradient reaches the flame surface only the centerline is exposed to the stoichiometric mixture fraction and locally maintains the planar flame speed and reaction rate. Above this point the mixture is fuel rich, and below fuel lean. As a result, these regions of non-unity equivalence ratio burn less, the reaction rate drops, and the local flame speed is reduced. The excess fuel and oxidizer then combine behind the premixed flame along the stoichiometric surface and burn in a trailing diffusion flame. Thus the "triple" flame refers to the fuel-rich premixed flame, the fuel-lean premixed flame, and the trailing diffusion flame.

In addition to the change in structure that occurs when the planar premixed flame is subjected to a mixture fraction gradient, the propagation velocity of the flame increases as observed in Fig. 2. In order to study the triple flame in further detail, a method of stabilizing the flame in the computational domain is needed. We accomplish this by calculating the relative progression velocity of iso-scalar surfaces. This method results from equating the transport equation for a scalar variable Y:

$$\rho \frac{DY}{Dt} = \frac{\partial}{\partial x_i} \left(\rho \mathcal{D} \frac{\partial Y}{\partial x_i} \right) + \dot{w}_Y$$

with the Hamilton-Jacobi equation for the scalar field (Kerstein *et al.* 1989):

$$\rho \frac{DY}{Dt} = \rho V |\nabla Y|.$$

Solving for the relative progression velocity of the iso-concentration surface, V, we obtain:

$$V = \frac{1}{\rho |\nabla Y|} \frac{\partial}{\partial x_i} \left(\rho \mathcal{D} \frac{\partial Y}{\partial x_i} \right) + \frac{1}{\rho |\nabla Y|} \dot{w}_Y$$

This relation is evaluated on the centerline in the preheat zone and subtracted from the local fluid velocity, giving the correction to be applied at the inlet. If one were

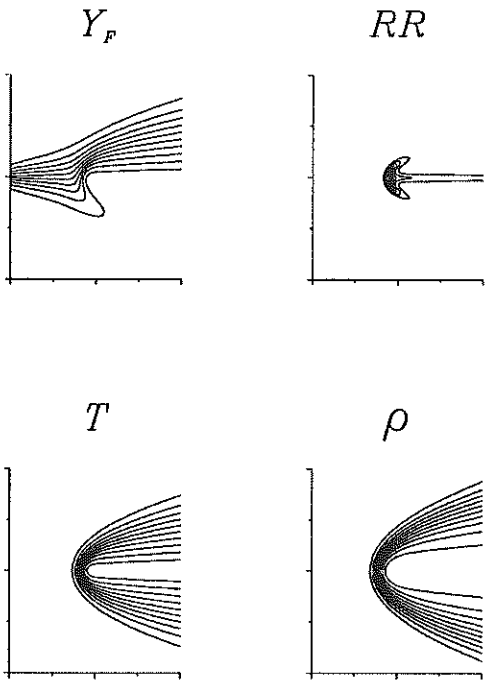

FIGURE 3. Contours of mass fraction, reaction rate, temperature, and density for a stabilized triple flame.

to apply this correction at the inlet alone, then changes to the flame would only occur after the convective time required to reach the flame, which is both time consuming and can also introduce stability problems. A more efficient method is to apply the correction to all points in the flow as a Gallilean transformation, such that the steady-state situation is quickly reached.

Some care must be taken in choosing the size of the computational domain. Because the triple flame redirects the flow laterally, the top and bottom boundaries must be moved far enough from the stoichiometric conditions so that the viscous boundary conditions do not affect the flame speed. To avoid this problem, an unevenly spaced grid is used in the lateral direction where points are clustered about the stoichiometric line so that the lateral boundaries can be moved far away from the flame. In addition, all results presented here were run on different sized domains to check that the size of the computational domain does not play a role in the flame speed.

2. Accomplishments

To begin the investigation of heat release effects on triple flames, we first describe some general characteristics of triple flames. We have briefly described the structure of triple flames in the time sequence of Fig. 2, where the flame propagates relative to the inflow. Fig. 3 shows similar contours, in addition to the temperature and density fields, for a triple flame stabilized in the computational domain. The effects of heat release are clearly seen in the temperature and density plots, where the temperature rises and density decreases behind the premixed wings of the flame, along with the effects of the nonuniform mixture fraction gradient, where the temperature and density fields display lateral variations.

Lateral diffusion of temperature and species plays an important role in triple flames. Behind the premixed wings of the flame, heat is conducted away from the stoichiometric line. This conduction is important because, unlike one-dimensional flames with an infinite heat reservoir in the burned regions, heat from the triple flame is convected to regions which do not contribute to flame propagation. Thus, quenching is more likely to occur if enough heat is conducted laterally away from the flame. Lateral diffusion of species is also important and is responsible for the diffusion wing of the flame.

Another way to determine the role of lateral diffusion is to compare one-dimensional profiles of different quantities along the stoichiometric line of the triple flame with those of the one-dimensional flame used to initialize the simulations. These plots are presented in Fig. 4 where the quantities are scaled by their minimum and maximum values of the one-dimensional flame. The behavior of all quantities is similar up to, and somewhat behind, the maximum reaction rate. Behind the premixed reaction zone, we observe that only the density profile is roughly equal in both cases. We observe a drop in temperature and an increase in fuel (and also oxidizer) mass fraction relative to the one-dimensional case. The change in reaction rate is dominated by the increased mass fractions of the reactants, and consequently an increase in the reaction rate is observed behind the flame. This reaction rate corresponds to the burning in the trailing diffusion flame and is a sizable percentage of the maximum reaction rate. These differences between the one-dimensional profiles and profiles through the stoichiometric line in the triple flame become larger as we increase the mixture fraction gradient.

Up to this point we have not included the velocity in our analysis. We have postponed this until the next section since the velocity field in the triple flame is quite different than in the planar flame and requires a detailed investigation.

2.1 Effects of heat release on flame propagation

We now turn our attention to studying the effect of heat release on the triple flame and, in particular, how this affects the propagation velocity. The analytical work of Dold 1989 and Hartley and Dold 1991 provide estimates of the triple-flame speed for weak ($\beta\partial Z/\partial y \to 0$) and moderate ($\beta\partial Z/\partial y \sim O(1)$) values of the mixture fraction gradient under the assumption of zero heat release. They find that the flame speed is greatest for zero mixture fraction gradient, corresponding to a planar flame, and then decreases as the mixture fraction gradient increases. This is in

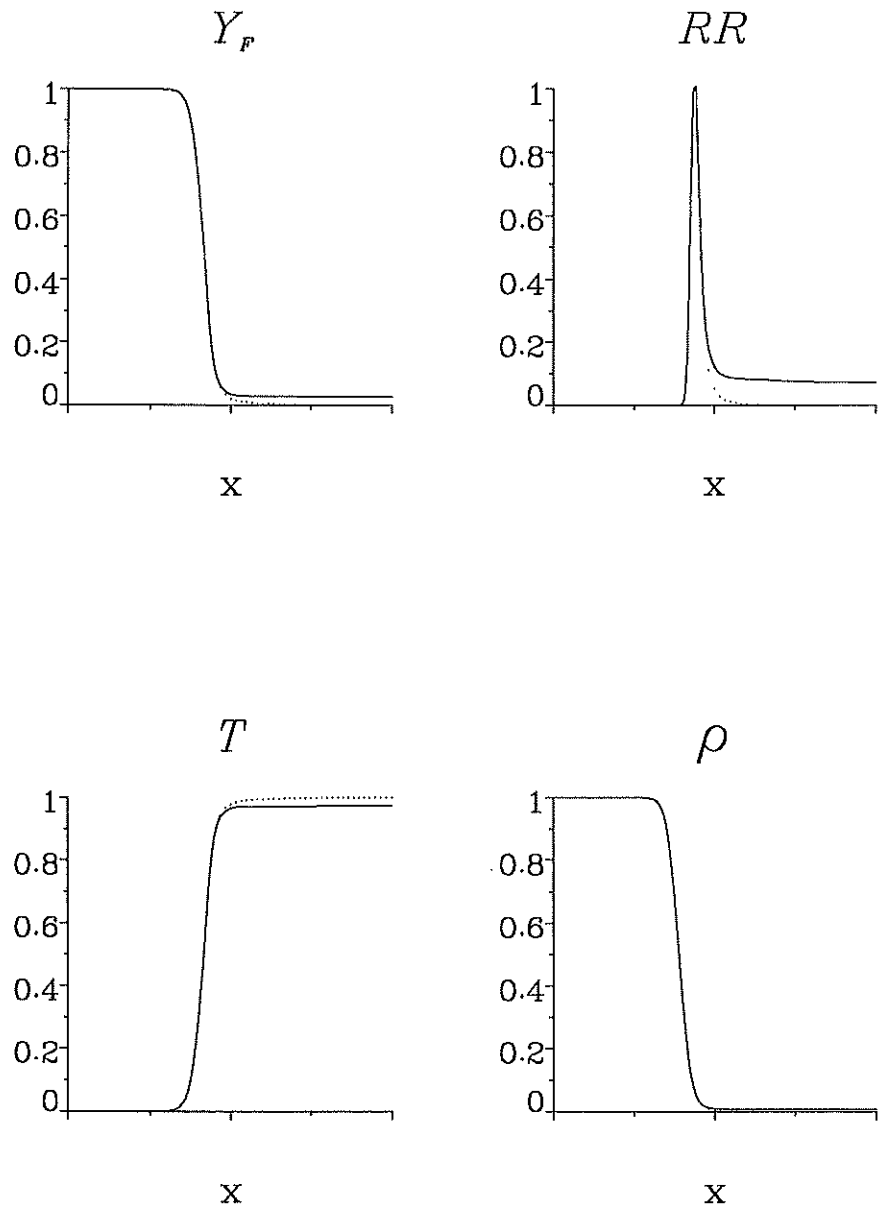

FIGURE 4. Profiles of various quantities in a one-dimensional flame (----) and along the centerline of the triple flame (———). Lateral heat conduction reduces the temperature of the triple flame, and diffusion of fuel and oxidizer increase the reaction rate behind the premixed flame.

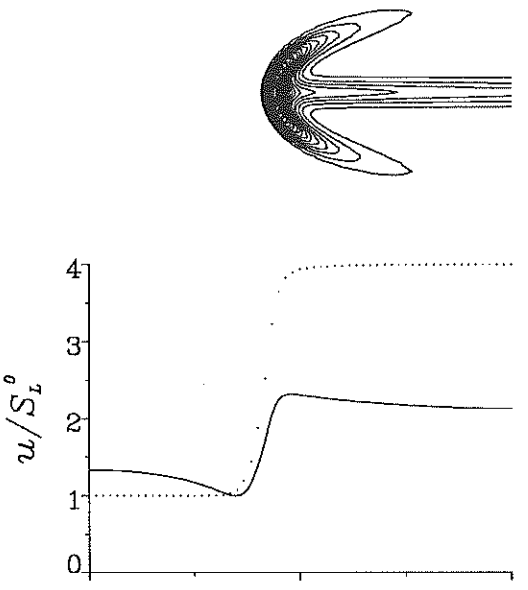

FIGURE 5. Contour lines of the reaction rate along with the horizontal velocity component along the stoichiometic or symmetry line for a stabilized triple flame (———) and planar premixed flame (----). For the triple flame the velocity reaches a minimum just in front of the flame which is close the the premixed planar flame velocity. Upstream of the flame, however, the velocity is larger.

contrast to the change in flame speed we observe from the time sequence in Fig. 2. The discrepancy lies in the assumptions concerning heat release. To investigate this further, we examine the velocity field along the centerline of the triple flame in Fig. 5. Here we observe that, in addition to the rise in velocity through the flame, the horizontal velocity component reaches a minimum before the flame. The velocity at this minimum is close to the planar laminar flame speed, and far upstream the velocity is larger. Therefore it is necessary to distinguish these two velocities. The local flame speed is important in terms of chemical reaction, whereas the upstream or far-field flame speed is identified with the propagation of the entire structure, U_F.

The mechanism responsible for this velocity difference can be seen in the sketch of Fig. 6. Here we examine the velocity vectors before and after they pass through the flame surface. In cases with heat release, the component of the velocity perpendicular to the flame increases across the surface, whereas the tangential component remains unchanged. The jump in the perpendicular velocity component results in a bending of the velocity vector towards the centerline. This redirection of the flow is accommodated by the divergence of the streamlines ahead of the flame, resulting in

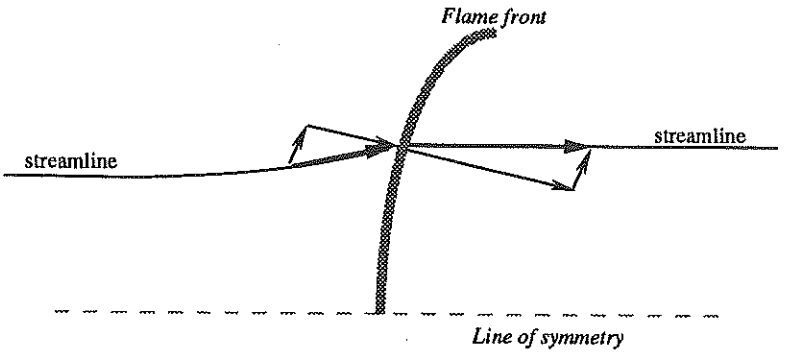

FIGURE 6. Mechanism responsible for increased flame speeds. Due to heat release the normal velocity across the flame is increased, whereas the tangential component remains unchanged. This redirection of flow towards the centerline causes the streamlines to diverge in front of the flame, resulting in a decrease in the flow velocity in front of the flame.

the decrease of the velocity observed in Fig. 5. Since the local flame speed along the stoichiometric line is near S_L^0, the flame can be stabilized only if the flow speed at this point remains at this value, which requires an increase in the upstream velocity. Note than in absence of heat release, there is no flow redirection across the flame, and therefore the far-field and local flame speeds are equal.

2.2 Effect of mixture fraction gradients

In their previous analytical work, Dold 1989 and Hartley and Dold 1991 observed a large effect of the mixture fraction gradient on the triple-flame propagation. Due to the effects of flame curvature, they observed a decrease in the flame speed as the mixture fraction gradient increases or equivalently the mixing thickness decreases. Thus for zero heat release cases the planar premixed flame represents an upper limit for the flame speed.

For cases with heat release, locally these same arguments still apply, however the far-field flame speed is much more affected by heat release than by flame curvature. This is depicted in Fig. 7, where the far-field flame speed, U_F/S_L^0, and the local flame speeds are plotted versus the nondimensional mixing thickness or Damköhler number. Here we see that, in agreement with the zero heat release analysis, the local flame speeds remain of the order of S_L^0, decreasing slightly below this value for small values of the mixing thickness. Also plotted in this figure is the difference between the local and far-field velocities. This difference eliminates the change in local conditions, and is therefore a true measure of the effect of heat release. As one can see from Fig. 7, this difference increases as the mixing thickness becomes

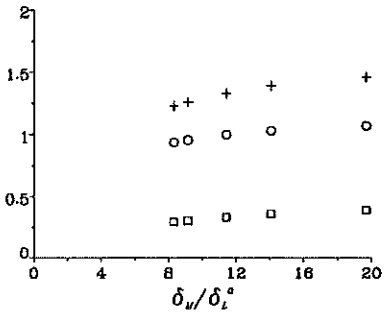

FIGURE 7. Far-field flame speed(+), local flame speed(o), and their differences(□) as a function of the local mixing thickness. All flame speeds are normalized by S_L^0, and for all cases $\alpha = 0.75$.

larger.

The reason for the increased effect of heat release as the mixing thickness becomes larger can be explained by Fig. 8. In Fig. 8 we plot the streamfunction through two flames with different mixing thicknesses. Since the maximum reaction rate is at the same streamwise location, we can superpose the two streamline patterns to determine how the flow redirection differs in these two cases. At streamwise locations near the maximum reaction rate and close to the stoichiometric line the two cases are similar. As we progress farther downstream, the case with the smaller mixing thickness spreads more laterally due to the greater burning in the diffusion flame. As we move laterally to regions further from stoichiometric conditions, the deflections of the streamlines away from the stoichiometric line become greater for the larger mixing thickness case. Recall that the mechanism for increased far-field flame speed relies on the acceleration of the normal velocity component through the flame. The local velocity jump across the flame is strongly related to the local reaction rate, which is in turn affected by the local mixture fraction. Thus, the distribution of the reaction rate along the premixed wings becomes an important characteristic and is the reason for the different streamline pattern farther from stoichiometric conditions. For small mixing thicknesses, the reaction rate drops off quickly as one moves away from stoichiometric conditions. For larger mixing thicknesses the reaction rate remains stronger as one moves along the premixed wings, and thus the redirection in the flow is more pronounced.

2.2.1 Small mixing thicknesses and resistance to quenching

For small values of the mixing thickness one might expect quenching to occur. Quenching would result from the lateral conduction of heat away from the flame. In previous analytical work (*cf.* Hartley and Dold 1991), however, quenching was not observed. Under the assumption of zero heat release, quenching was present

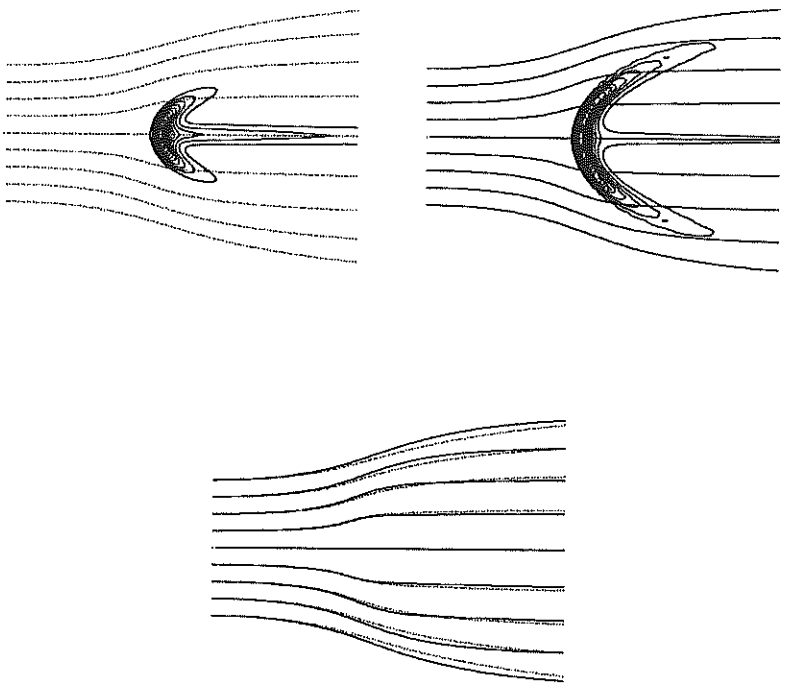

FIGURE 8. Streamlines for flames with small (left,- - - -) and large (right,———) mixing thicknesses. The streamlines are superposed beneath.

only when the flame was subjected to an external strain field (Dold *et al.* 1991). Kioni *et al.* 1993 have simulated triple flames under external strain and have found negative propagation velocities, or an extinction front, to occur when the mixing thickness is small enough, once again under the assumption of zero heat release. In our present study, therefore, we do not expect quenching to occur since no *external* strain is present. Furthermore, in cases with heat release the resistance to quenching is enhanced. This added resistance to quenching occurs as the flame-generated straining motion which creates the reduction in the horizontal velocity also decreases the effective mixture fraction gradient in front of the flame and, therefore, limits how small the effective Damköhler number can become in Fig. 7. This reduction in the local mixture fraction gradient is observed in Fig. 9. Here the mixture fraction gradient along vertical slices is taken at the inlet and on a slice through the maximum reaction rate. The mixture fraction gradient is everywhere reduced by diffusion, but near stoichiometric conditions the effect of the heat release-induced strain on the mixture fraction gradient is dominant.

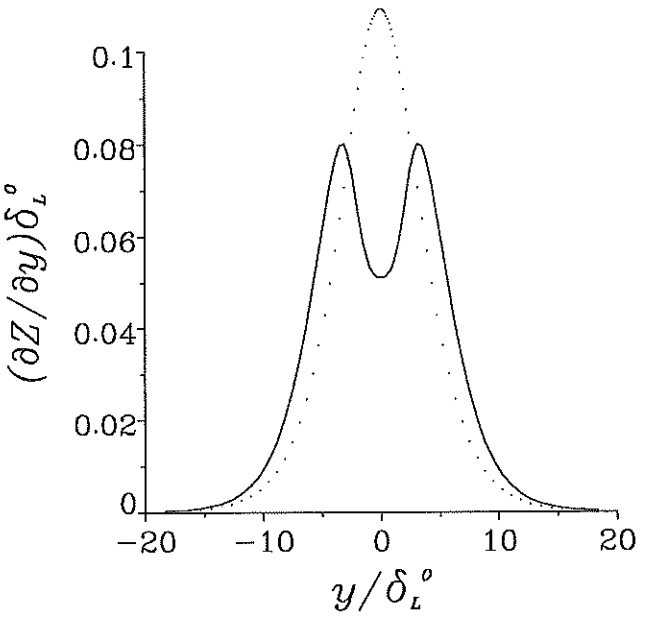

FIGURE 9. Vertical mixture fraction gradient profile at the inlet (·····) and on the vertical line passing through the maximum reaction rate (———).

2.2.2 Large mixing thicknesses and scaling laws

We have seen that for the range of mixing thicknesses considered in this study, as we increase the mixing thickness the propagation speed increases. We expect that for very large mixing thicknesses, where $\delta_M/\delta_L^0 \gg 1$, the flame speed reaches some asymptotic value.

We can derive an estimate of the flame speed by considering conservation relations applied to several locations along the stoichiometric line, shown in Fig. 10. These locations are: (1) far upstream, (2) immediately preceding the flame, (3) immediately following the flame, and (4) far downstream. For large mixing thicknesses, the flow in the immediate vicinity of the flame is nearly one-dimensional. Thus between stations (2) and (3) we can apply the Rankine-Hugoniot relations:

$$\rho_2 u_2 = \rho_3 u_3 \tag{1}$$

$$P_2 + \rho_2 u_2^2 = P_3 + \rho_3 u_3^2 \tag{2}$$

On either side of the flame the density can be taken as constant,

$$\rho_1 = \rho_2; \quad \rho_3 = \rho_4$$

so along the stoichiometric streamline we have

$$P_1 + \frac{1}{2}\rho_1 u_1^2 = P_2 + \frac{1}{2}\rho_2 u_2^2 \tag{3}$$

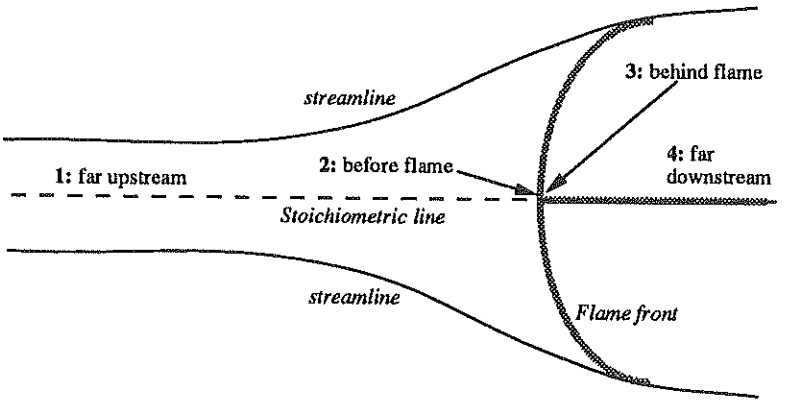

FIGURE 10. Triple flame for large mixing thicknesses. Propagation speed can be determined using conservation relations along the stoichiometric (dashed) line at stations 1-4, and also in the streamtube traced by the thin solid lines.

$$P_3 + \frac{1}{2}\rho_3 u_3^2 = P_4 + \frac{1}{2}\rho_4 u_4^2 \tag{4}$$

We identify the flow velocity in front of the triple-flame along the stoichiometric surface as the planar premixed flame speed:

$$u_2 = S_L^0$$

thus we are interested in determining u_1/u_2. In addition to the above relations we need to apply integral conservation laws. We choose a control volume which connects the upstream and downstream locations by streamlines which "touch" the edges of the premixed flames. If we denote the thickness of the control volume at any location by δ, then for mass conservation we have:

$$\rho_1 u_1 \delta_1 \sim \rho_4 u_4 \delta_4 \tag{5}$$

where as a first approximation we have assumed u_4 is constant behind the flame far downstream.

Combining these conservation relations and solving for u_1/u_2 we have:

$$\left(\frac{u_1}{u_2}\right)^2 = \frac{\left(\frac{\rho_1}{\rho_4} - 1\right)}{\frac{P_1 - P_4}{\frac{1}{2}\rho_1 u_1^2} + 1 - \frac{\rho_1}{\rho_4}\left(\frac{\delta_1}{\delta_4}\right)^2} \tag{6}$$

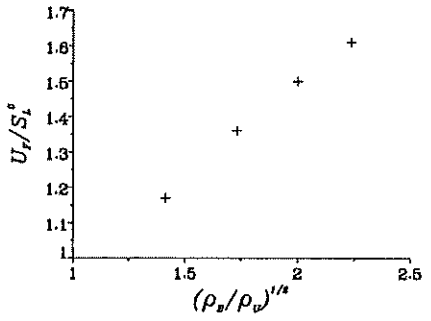

FIGURE 11. Flames speed ratio versus density ratio in simulation.

Equation 6 thus provides us with the propagation speed relative to the planar flame speed as a function of the density, pressures, and thicknesses at stations (1) and (4). However, we would like to have this expression in terms of the densities alone. So, we need an integral form for momentum conservation over the control volume. If we denote the average pressure along the control volume streamlines as P_s, then the global momentum relation is:

$$P_1\delta_1 + \rho_1 u_1^2\delta_1 + P_s(\delta_4 - \delta_1) = P_4\delta_4 + \rho_4 u_4^2\delta_4 \tag{7}$$

If we further make assumption that $P_1 = P_4 = P_s$, then Eq. 7 gives:

$$\rho_1 u_1^2\delta_1 = \rho_4 u_4^2\delta_4$$

which after using the overall mass conservation equation, we obtain:

$$u_1 = u_4; \quad \frac{\delta_1}{\delta_4} = \frac{\rho_4}{\rho_1}$$

Substituting this into Eq. 6 along with the equal pressure assumption gives:

$$\frac{U_F}{S_L^0} = \frac{u_1}{u_2} \sim \left(\frac{\rho_1}{\rho_4}\right)^{1/2} \tag{8}$$

Numerically we cannot simulate flames with the length-scale ratios required in the above formulation; however, we do observe the scaling behavior in Eq. 8 for our simulations with large mixing thicknesses, shown in Fig. 11.

3. Future work

In this study we have investigated one possible flame structure that can occur in partially-premixed conditions. We have established the role that heat release plays

on this flame and its propagation assuming rather benign conditions for the flow and chemistry. Just as we have relaxed the assumption of zero heat release used in previous studies, in the future we must also relax the assumptions presently made concerning the flow field and chemical reaction mechanism.

The assumption of uniform parallel flow has enabled us to determine how the flow is modified by heat release, but is too simple a model to describe the behavior of flames in turbulent combustion. As a first step towards understanding flame stabilization in turbulent combustion, the response of triple flames to vortices was examined in Veynante *et al.* 1994, where triple flames were found to be more robust than nonpremixed flames under similar circumstances. However, even before we consider turbulent or vortical flows, there are several questions one can ask about flame behavior in simpler flows.

In many practical applications reactants are mixed in jet flows, where the fuel and oxidizer streams have different velocities. In such cases the lateral position of the flame, i.e. whether it lies in the fuel or oxidizer stream, can greatly affect stabilization. There are several parameters that can change the flame position. Stoichiometry clearly has a large affect on flame positioning. The effects of stoichiometry on triple-flame structure has been investigated for zero heat release flames by Dold 1989, but how this is coupled with heat release has yet to be determined. Non-unity Lewis numbers can also modify flame positioning. A method for simulating non-unity Lewis numbers in diffusion flames has been developed by Liñán *et al.* 1994, where the position of the diffusion flame in a shear layer was found to play a large role in the overall dynamics. Non-unity Lewis numbers modify more that the flame position, however. Buckmaster and Matalon 1988 showed for zero heat-release flames that the triple-flame structure can be altered dramatically where one of the premixed wings can point into the oncoming flow. Lewis number effects can also modify the flame propagation, and this is expected to have a very pronounced effect due to the large curvature inherent to the triple-flame structure.

Aside from including more complicated flow, stoichiometry, and Lewis number effects in studies of partially-premixed combustion, there are other modifications that can be implemented. We have shown in this study that the distribution of the reaction rate along the premixed wings of triple flames greatly affects the flame propagation. Because of this, flamability limits included in the chemical mechanism can be introduced. Extending the chemical model to include multiple steps is also desirable in certain cases. This is especially true if one is interested in NO_x formation during ignition. Because NO_x formation occurs during non-equilibrium combustion, multi-step chemistry is necessary for investigating pollutant formation.

Acknowledgments

The author would like to thank T. Mantel, J.-M. Samaniego, and L. Vervisch for their helpful suggestions throughout this study. A. Liñán, T. Poinsot, and D. Veynante also provided helpful information and discussions during the CTR summer program.

REFERENCES

BUCKMASTER, J. & MATALON, M. 1988 Anomalous Lewis number effects in tribrachial flames. *Twenty-second Symposium (International) on Combustion,* The Combustion Institute, p. 1527.

DOLD, J. W. 1989 Flame propagation in a nonuniform mixture: analysis of a slowly varying triple flame. *Combust. & Flame.* **76,** 71.

DOLD, J. W., HARTLEY, L. J. & GREEN, D. 1991 Dynamics of laminar triple-flamelet structures in non-premixed turbulent combustion. *Dynamical Issues in Combustion Theory.* Springer-Verlag, 83.

HARTLEY, L. J. & DOLD, W. 1991 Flame propagation in a nonuniform mixture: analysis of a propagating triple-flame. *Comb. Sci. & Tech.* **80,** 23.

KERSTEIN, A. K., ASHURST, WM. T., & WILLIAMS, F. A. 1988 Field equation for interface propagation in an unsteady homogeneous flow field. *Phys. Rev. A.* **37,** 2728.

KIONI, P. N., ROGG, B., BRAY, K. N. C. & LIÑÁN, A. 1993 Flame spread in laminar mixing layers: the triple flame. *Combust. & Flame.* **95,** 276.

LELE, S. 1992 Compact finite difference schemes with spectral-like resolution. *J. Comp. Phys.* **103,** 16.

LIÑÁN, A. 1994 Ignition and flame spread in laminar mixing layers. *Combustion in high speed flows.* ed. Buckmaster, Jackson, and Kumar, Kluwer Acad. Pub., 461.

LIÑÁN, A., ORLANDI, P., VERZICCO, R., & HIGUERA, F. J. 1994 Effects of non-unity Lewis numbers in diffusion flames. *Proceedings of the 1994 Summer Program.* Center for Turbulence Research, NASA Ames/Stanford University.

MCMURTRY, P. A., RILEY, J. J., & METCALFE, R. W. 1989 Effects of heat release on the large-scale structure in turbulent mixing layers. *J. Fluid Mech.* **199,** 297.

PETERS, N. 1983 Local quenching due to flame stretch and non-premixed turbulent combustion. *Comb. Sci. & Tech.* **30,** 1.

PETERS, N. 1994 The modeling of combustion and pollutant formation in engine flows. *Proceedings from a small conference.*

PHILLIPS, H. 1965 Flame in a buoyant methane layer. *10th International Symposium on Combustion.* p. 1277.

POINSOT, T. & LELE, S. 1992 Boundary conditions for direct simulations of compressible viscous flows. *J. Comp. Phys.* **101,** 104.

RÉVEILLON, J., DOMINGO, P., & VERVISCH, L. 1994 Autoignition in non-uniform mixture. To be published.

TROUVE, A. 1991 Simulation of flame-turbulence interaction in premixed combustion. *Annual Research Briefs 1991.* CTR, Stanford University/Nasa Ames.

VERVISCH, L., KOLLMANN, W., & BRAY K. N. C. 1994 Pdf modeling for premixed turbulent combustion based on the properties of iso-concentration surfaces. *Proceedings of the 1994 Summer Program.* CTR, NASA Ames/Stanford University.

VEYNANTE, D., VERVISCH, L., POINSOT, T., LIÑÁN, A. & RUETSCH, G. 1994 Triple flame structure and diffusion flame stabilization. *Proceedings of the 1994 Summer Program.* CTR, NASA Ames/Stanford University.

WILLIAMS, F. A. *Combustion Theory* Addison-Wesley, NY, 1986.

WRAY, A. A. Private communication.